

Controlling multistability in coupled systems with soft impacts

P. Brzeski^a, E. Pavlovskaja^b, T. Kapitaniak^a, P. Perlikowski^{a,*}

^a*Division of Dynamics, Lodz University of Technology, Stefanowskiego 1/15, 90-924 Lodz, Poland*

^b*Centre for Applied Dynamics Research, School of Engineering, University of Aberdeen, AB24 3UE, Aberdeen, Scotland*

Abstract

In this paper we present an influence of discontinuous coupling on the dynamics of multistable systems. Our model consists of two periodically forced oscillators that can interact via soft impacts. The controlling parameters are the distance between the oscillators and the difference in the phase of the harmonic excitation. When the distance is large two systems do not collide and a number of different possible solutions can be observed in both of them. When decreasing of the distance, one can observe some transient impacts and then the systems settle down on non-impacting attractor. It is shown that with the properly chosen distance and difference in the phase of the harmonic excitation, the number of possible solutions of the coupled systems can be reduced. The proposed method is robust and applicable in many different systems.

Keywords:

Multistability, Discontinuous coupling, Control

1. Introduction

The interaction between impacting systems is nowadays extensively investigated. In many systems such as tooling machines, gear boxes, heat exchangers and backlash gear the motion of some elements is limited by a barrier. There are many impact models which give the relations between the interacting system elements. Generally, they can be divided into two groups, i.e., the hard and soft impacts [1, 2, 4, 3]. The hard impacts are modeled by the restitution coefficient [6, 7, 5]. In this approach the time of contact is infinitely small and the exchange of energy is instantaneous. The second approach (soft impact) assumes the finite, nonzero contact time and a penetration of the base by the colliding body. Hence, the contact is modeled as a linear [8, 9, 10], Hertzian [11, 12] or other nonlinear [13] spring and viscous damper. The separate equations of motion describe the in-contact and out-of-contact dynamics.

The numerous works have been devoted to phenomena induced by the impacts. The bifurcation scenarios and implication of grazing events are quite well understood [14, 15, 16, 17]. There are a few studies which focus on the systems where impacts between coupled oscillators are transient. Blaziejczyk-Okolewska *et. al.* [18] show that impacting systems can synchronize (via the exchange of energy during the contact) in anti-phase on chaotic attractor. The impacts can be considered as a discontinuous transient coupling which disappears once the interacting systems reach the synchronous solutions.

The phenomenon of synchronization is commonly encountered in non-linear systems [19, 20, 21]. Generally, in coupled mechanical systems one can observe two types of synchronous motion, i.e., the complete and the phase synchronization [22, 23, 24, 25]. As the coupling between mechanical oscillators (two directly interacting bodies or via spring, damper or inerter) is always bidirectional; when systems are completely synchronized the value of coupling force is equal to zero, and only if common motion is perturbed the systems once again start to interact (note that for non-mechanical systems it is not always true). This is the straightforward analogy to the above mentioned discontinuous transient coupling via impacts, where

*Corresponding author

Email address: przemyslaw.perlikowski@p.lodz.pl (P. Perlikowski)

the perturbation of stable non-impacting solution leads to the appearance of transient impacting motion (coupling).

In this paper we demonstrate the idea and present solution to reduce complexity via transient impacts. We consider systems of two identical oscillators and assume that interaction between them occurs through soft impacts. When the systems are uncoupled we observe multiple stable attractors for each subsystem. Using a piecewise transient coupling to another identical subsystem we can change the number of stable attractors and, in many cases, specify on which attractor both systems settle.

The paper is organized as follows. In Section 2 we consider a simple model which is used to demonstrate the main idea of our approach and define the notations introduced to describe existing periodic states. In the next section we present and describe the how via discontinuous coupling we can decrease number of solutions in the complex systems with many co-existing periodic solutions of different type. The possible coexistence of impacting and non-impacting solutions is discussed in Section 4. Finally, in Section 5 the conclusions are given.

2. Duffing systems

In this section we show the main idea of our approach using a simple example. First, the considered model is introduced and the notations used to classify the existing solutions are defined. Then, we present the results of the numerical analysis.

2.1. Model of the system

The system considered in this subsection consists of two identical Duffing oscillators shown in Figure 1. Oscillators in their steady states (at rest) are separated by the distance d , and the impacts which could occur between them are of the soft type due to the presence of a spring with stiffness k_c and a viscous damper with damping coefficient c_c . Two Duffing oscillators have masses M each and are damped by viscous dampers with damping coefficient c . The spring connecting each oscillator to the wall is nonlinear and of hardening type, where both stiffness coefficients are positive: $k_1 > 0$ and $k_2 > 0$. Both Duffing systems are driven by harmonic forces with the amplitude F and the frequency ω but there is a phase shift between these forces. Forcing of the first oscillator has fixed phase (equal to zero) while for the second one there is a phase shift φ which is used as a control parameter ($\varphi \in (0, 2\pi)$).

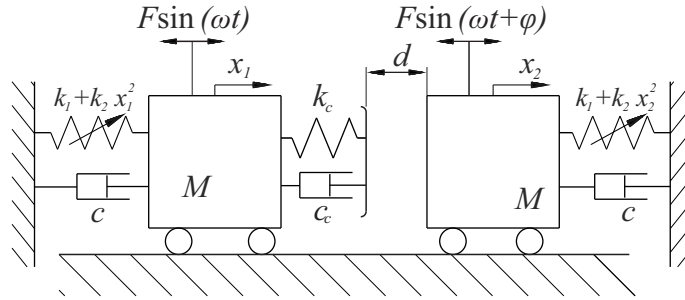


Figure 1: Model of two discontinuously coupled Duffing oscillators.

The whole system is described by the following equations of motion:

$$M\ddot{x}_1 + k_1x_1 + k_2x_1^3 + c\dot{x}_1 + F_C = F \sin(\omega t) \quad (1)$$

$$M\ddot{x}_2 + k_1x_2 + k_2x_2^3 + c\dot{x}_2 - F_C = F \sin(\omega t + \varphi) \quad (2)$$

where F_C describes the forces generated by the discontinuous coupling and is given by the formula:

$$F_C = \begin{cases} 0 & \text{for } x_1 - x_2 < d \\ k_c ((x_1 - x_2) - d) + c_c (\dot{x}_1 - \dot{x}_2) & \text{for } x_1 - x_2 \geq d \end{cases} \quad (3)$$

The values of the parameters are as follows: $M = 1.0 [kg]$, $k_1 = 1.0 [\frac{N}{m}]$, $k_2 = 0.01 [\frac{N}{m^3}]$, $c = 0.05 [\frac{Ns}{m}]$, $F = 1.0 [N]$, $\omega = 1.3 [\frac{1}{s}]$, $k_c = 8.0 [\frac{N}{m}]$, $c_c = 10.0 [\frac{Ns}{m}]$. Distance between system d and phase shift in excitation φ are controlling parameters. Introducing dimensionless time $\tau = t\omega_1$, where $\omega_1 = 1 [\frac{1}{s}]$, reference length $l_r = 1.0 [m]$ and mass $m_r = 1 [kg]$ we transform the equations (1) – (3) into dimensionless form in which dimensional parameters are replaced by the following non-dimensional parameters:

$$M' = \frac{M}{m_r}, k'_1 = \frac{k_1 l_r}{m_r \omega_1^2}, k'_2 = \frac{k_2 l_r^2}{m_r \omega_1^2}, c' = \frac{c}{m_r \omega_1}, F' = \frac{F}{m_r l_r \omega_1^2}, \omega' = \frac{\omega}{\omega_1}, k'_c = \frac{k_c l_r}{m_r \omega_1^2}, c'_c = \frac{c_c}{m_r \omega_1}, d' = \frac{d}{l_r}.$$

We perform transformation to the dimensionless form in the way that enables to hold the values of parameters, hence: $M' = 1.0$, $k'_1 = 1.0$, $k'_2 = 0.01$, $c' = 0.05$, $F' = 1.0$, $\omega' = 1.3$, $k'_c = 8.0$, $c'_c = 10.0$. For simplicity all of the primes used in definitions of dimensionless parameters will be omitted hereafter in the analysis.

2.2. Notations for the periodic solutions

We introduce the notations that enable to describe all periodic states of two impacting oscillators, hence we can classify all solutions that can occur in the considered system. To recall, we assume that the left (first) system is a reference system, hence its phase of excitation and position are fixed while for the right (second) system the phase of excitation φ can vary in the range from 0 to 2π and the oscillator's position can be changed to decrease or increase the distance d . The solution of the left oscillator is described in the following way:

$$L_{pl}^{nl}$$

where: nl is the number of the attractor (in case of multiple attractors of isolated oscillator) and pl is the period of given attractor in respect to the period of excitation (we assume that solutions are periodic). Similarly, the solution of the right oscillator is given by:

$$R_{pr}^{nr}$$

where: nr is the number of the attractor (in case of multiple attractors of isolated oscillator), pr is the period of given attractor. To define the solution of the interacting oscillators system we will use the following notations:

$$L_{pl}^{nl} R_{pr-s}^{nr}.$$

where s is the shift in phase between the systems given by an integer number when the period of solution is longer than the period of excitation i.e., $s = 1$ for 2π shift and so on.

The best example to describe the importance of s is a case when we have two identical systems both with the same period-2 solution (i.e. their response periods are twice longer than the period of excitation). In Poincaré map, for both systems, we observe two dots. Let's assume that the position of the first oscillator, at the sampling moment of time, is in one of the dots. Then, the second oscillator can be either in the same position ($s = 0$) or in the second dot when its phase is shifted by one period of excitation ($s = 1$). Number of possible shifts is equal to the greatest common divisor (gcd) of both systems solutions' periods. Let us now consider an example where both oscillators have period-2 and period-5 co-existing solutions. If the first oscillator is on period-2 solution and the second one is on period-5 solution only one configuration is possible because $\text{gcd}(2, 5) = 1$, so we have one possible value of $s = 0$. In the other case where both oscillators have period-4 and period-6 co-existing solutions, the $\text{gcd}(4, 6) = 2$, hence $s = 0$ or $s = 1$.

Figure 2 demonstrates these examples. In Figure 2(a) we show possible configuration for systems with periods 2 and 5. In this case the period of the whole system is equal to 10. The upper row shows the sequence of possible positions of the system with period 2 (1st or 2nd dot on Poincare map), while the lower

row presents the possible positions of the system with period 5 (1st to 5th dot on Poincare map). It is easy to see that along one period of the whole system all possible pairs of numbers are created, hence no more states can occur and any shift makes no difference. In Figure 2(b) we show the second example when two possible configurations for systems with periods 4 and 6. The first case for $s = 0$ (upper) where both system start from dot No. 1 (one in the lower and the upper row) and the second case for $s = 1$ when the first oscillator starts motion from dot No. 1 and the second system from dot No. 2. Analysing the graph we see that shifts $s = 0$ and $s = 1$ create all possible pairs of dots on Poincare map.

For example, if each oscillator has only one period-2 solution, the solutions of the interacting system can be described as $L_2^1 R_{2-0}^1$ and $L_2^1 R_{2-1}^1$. More examples and the detailed explanations for the possible solutions in the system with co-existing attractors are given in the following sections.

It should be noted that in our investigations we use the relative position of two oscillators on their attractors which depend on the phase shift of excitation φ . Therefore, in the plots each presented solution is marked as

$$L_{pl}^{nl} R_{pr-s}^{nr}(\varphi).$$

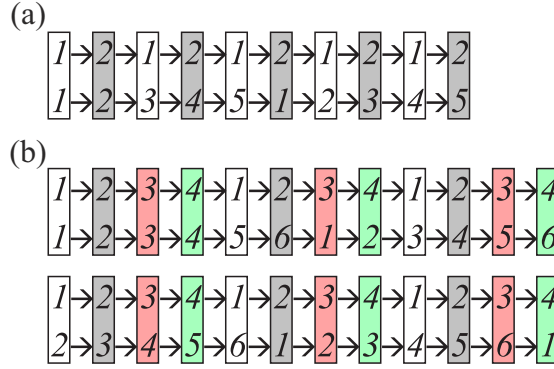


Figure 2: The possible combinations of the system states for (a) period-2 and period-5 solutions and (b) period-4 and period-6.

2.3. Possible non-impacting states of the considered system

After defining the notations we can continue the analysis of two Duffing systems introduced at the beginning of this section. For the assumed parameters single Duffing oscillator has two period-1 solutions with large and small amplitude, respectively. Their basins of attraction are shown in Figure 3, where the non-resonant solution with small amplitude is marked by No. 1 (orange basin) and the resonant solution with large amplitude by No. 2 (green basin). The basins' boundary is a smooth curve so it is clear which attractor is reachable for the given initial condition. All numerical calculations are performed using Runge-Kutta 4th order method with constant time step equal to $T/1440$, where T is period of excitation.

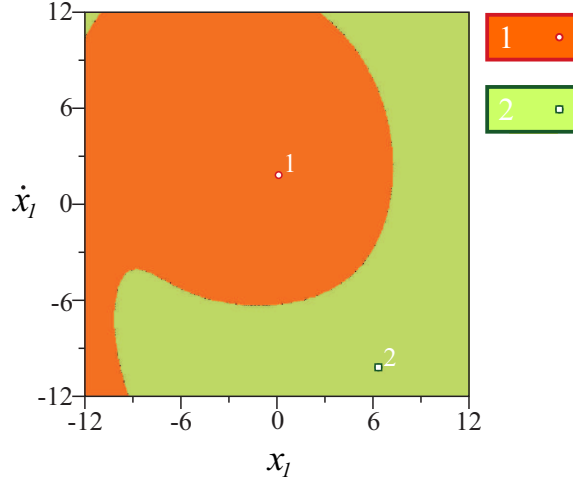


Figure 3: Basins of attraction for one Duffing oscillator. ($M = 1.0$, $k_1 = 1.0$, $k_2 = 0.01$, $c = 0.05$, $F = 1.0$, $\omega = 1.3$).

For two identical systems shown in Figure 1, trajectories of two coexisting period-1 solutions on the phase plane are presented in Figure 4 (a) for the following values of the system parameters ($M = 1.0$, $k_1 = 1.0$, $k_2 = 0.01$, $c = 0.05$, $F = 1.0$, $\omega = 1.3$). According to the introduced notation, the solution of the left system can be either the period-1 attractor with small amplitude (small loop) denoted by L_1^1 or the period-1 attractor with large amplitude (large loop) denoted by L_1^2 . The dots on small and large loops of the left oscillator's trajectories correspond to the maximum displacements which the oscillator could reach. When the left system is in the point L_1^1 the solution of the right system can be either on the small amplitude period-1 attractor represented by the dot on the small loop or on the large amplitude period-1 attractor (the dot on the large loop) - this corresponds to solutions $L_1^1 R_{1-0}^1(0)$ (red dot) or $L_1^1 R_{1-0}^2(0)$ (green dot). When the left system is in the point L_1^2 , the possible locations of the second oscillator are $L_1^2 R_{1-0}^1(0)$ (yellow dot) and $L_1^2 R_{1-0}^2(0)$ (black dot). Note that when the systems are on the different trajectories (the left on the small and the right on the large and vice versa) their positions are shifted in phase without the phase shift in excitation ($\varphi = 0$). The detailed scheme of solutions is shown in Figure 4 (b).

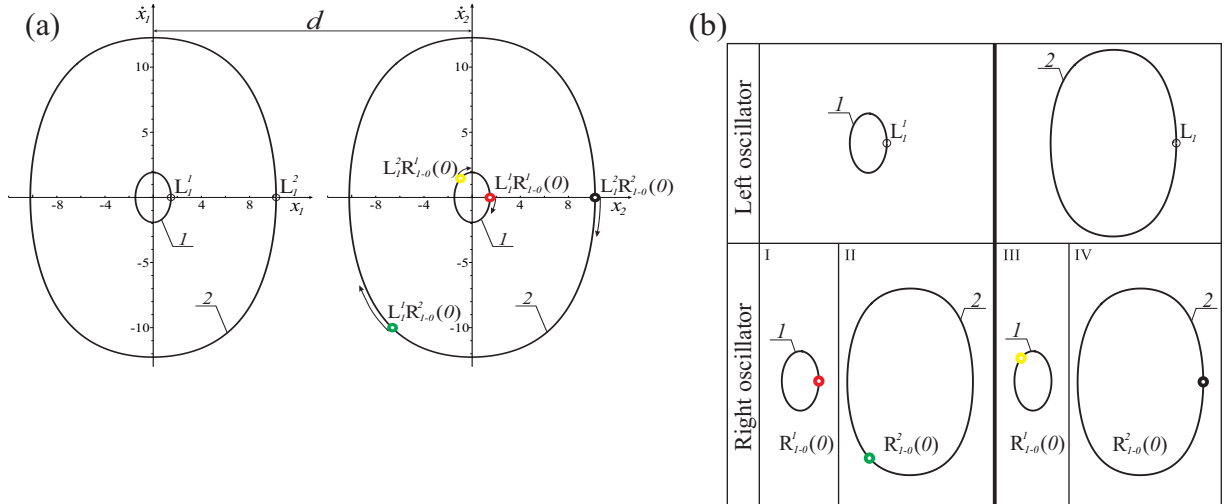


Figure 4: Possible attractors of two Duffing oscillators for in-phase forcing ($\varphi = 0$) (a) and four possible solutions of the system that consists of two Duffing oscillators (b). ($M = 1.0$, $k_1 = 1.0$, $k_2 = 0.01$, $c = 0.05$, $F = 1.0$, $\omega = 1.3$).

As we mention before, our controlling parameters are the phase shift of excitation φ and the initial distance between the oscillators. The current distance between the oscillators can be measured as $x_1 - x_2 - d$ and it depends on the relative position of each oscillator along the trajectory governed by the phase shift φ . Impact between the two oscillators occurs when the distance $x_1 - x_2 - d$ is zero or positive. The presence of impacts in the steady state response introduces new types of solutions in the combined system and depending on the values of d and φ destroys the combinations of period-1 solutions described earlier. In Figure 5(a) two parameters plot is presented showing the boundaries for which given combinations of period-1 solutions exist. Considered system has four possible combinations of the solutions and each of them is marked by a different colour. Solution $L_1^1 R_{1-0}^1(\varphi)$ disappears for all values of d and φ which are located below the red line on the graph. For $\varphi = 0$, the critical distance $d = d_{crit}$ is equal to zero because the oscillators are moving in phase, so no collision is possible (they are in contact and $x_1 = x_2$). For $\varphi = \pi$ oscillators move in anti-phase, hence the impact (destruction of given solution) occurs as soon as trajectories start to overlap.

To calculate the boundaries presented in Figure 5(a), the distance between two oscillators needs to be monitored. In Figures 5(b-d) the difference between the displacements of two oscillators $x_1 - x_2$ over one period of steady state motion for $L_1^2 R_{1-0}^2(\varphi)$ solution is shown for three different cases, i.e., $\varphi = \pi/4$, $\varphi = 3\pi/4$, and $\varphi = \pi$. The red triangle marks indicate the maximum difference between the displacements during one period of this solution. As the impact occurs when $x_1 - x_2 - d > 0$, choosing the critical distances d_{crit} for given phase shifts φ based on these maximum differences, i.e. (b) $d_{crit} = 7.44466$, (c) $d_{crit} = 18.66971$ and (d) $d_{crit} = 20.40519$, would guarantee that for any $d > d_{crit}$, there will be no collisions between two oscillators and therefore this type of solution will exist. For $d < d_{crit}$ the coupled systems interact and the solution is destroyed. Before oscillators settle down on the attractor we observe the transient dynamics due to non-identical initial conditions. However it does not influence the existence and stability of non-impacting solutions. As can be seen from these graphs, the critical distance d_{crit} is a function of the phase shift φ and is valid for given pair of solutions. In other words, given solution disappears when distance between oscillators becomes smaller then d_{crit} .

The graph shown in Figure 5(a) gives us a clear understanding of how the value of the phase shift φ influences the critical distance d_{crit} . As one can expect, the solution that remains stable for the lowest d is the case when two oscillators are both settled on the small attractors ($L_1^1 R_{1-0}^1(\varphi)$). Such solution exists for all values of d and φ above the red line. Two solutions where one system is on small attractor and the second one is on large attractor (yellow and green curves) disappear around $d = 10$ and are mirrored in respect to $\varphi = \pi$. The biggest influence of the shift phase on critical d_{crit} is observed for solution $L_1^2 R_{1-0}^2(\varphi)$ marked by black line. The Roman numbers printed in each area indicate which types of solutions are present there. All states are possible above all lines and crossing each line causes disappearance of one of them, finally below the red line no non-impacting solution is present. Those lines have been calculated based on trajectories of uncoupled systems and are borders of stability of given solution.

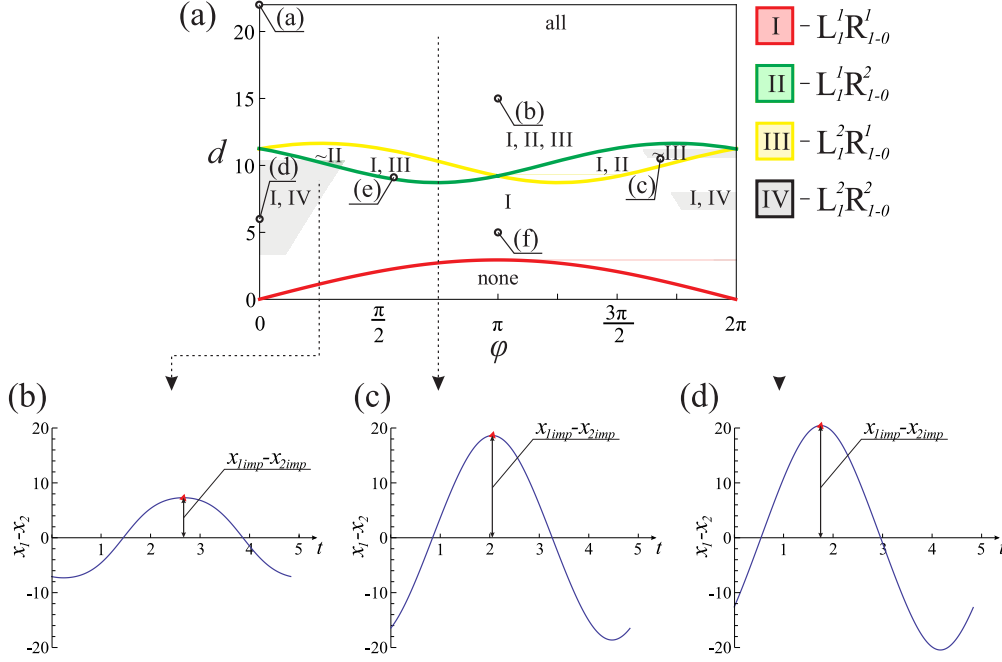


Figure 5: Possible solutions of the system that consists of two Duffing oscillators in the (d, φ) plane (a). Each type of solution is drawn with line of different color. Subplots (b-d) present trajectory traces of $L_1^2 R_{1-0}^2$ solution in plane (x_1, x_2) for different phase shifts φ , i.e., (a) $\varphi = \pi/4$; (b) $\varphi = 3\pi/4$; (c) $\varphi = \pi$. Red triangles represent the collision points. ($M = 1.0$, $k_1 = 1.0$, $k_2 = 0.01$, $c = 0.05$, $F = 1.0$, $\omega = 1.3$).

In Figure 6 we present six basins of attractions in plane (x_1, x_2) calculated for the initial velocities of oscillators fixed to zero, i.e., $\dot{x}_1 = \dot{x}_2 = 0.0$. As the full dimension of phase space is four (i.e. the complete set of initial conditions for the system includes two displacements and two velocities), it is difficult to visualize the basins of attraction for all possible initial states. Therefore, two dimensional cross-sections of the phase space are presented with two most relevant state variables as parameters. It is clear that in two dimensional projection each oscillator should be represented by one variable. In mechanical systems one can easily control and precisely impose the initial displacements, while such control is impossible or very difficult for the velocities. Therefore, in the current study the velocities of both systems were fixed as zero and only displacements are varied.

Each basin is computed for different φ and d to show that varying of the phase and the distance between two oscillators changes the number of coexisting solutions. Circles in Figure 5(a) marked by letters (a)-(f) correspond to values of φ and d for which the basins are calculated. Figure 6(a) shows basins for two oscillators calculated for in phase forcing ($\varphi = 0$) and $d = 22$, the boundaries are straight lines and there is no coupling between the systems. When we decrease the distance, oscillators start to interact and one can observe disappearance of one or more solutions. In Figure 6(b) computed for $\varphi = \pi$ and $d = 15.0$, three coexisting solutions are present (Nos. I, II and III). This corresponds to point (b) in Figure 5(a) (below the black line) in plane (φ, d) , hence the case where two systems are on big loops is destroyed. In Figure 6(c) one can observe three solutions (Nos. I, III and IV) - disappearance of $L_1^1 R_{1-0}^2$ (5.28). Two next plots correspond to set of parameters for which only two solutions are observed (see Figure 6(d,e)) and the last possibility with just one present solution is shown in Figure 6(f).

It is important to clarify the position of the points marking the different attractors in the Figure 6. As can be seen from this figure, in some cases the attractors shown do not belong to their own basin (i.e. yellow, green and black symbols in Figure 6(a)). This can be explained by the fact that the basins are calculated for the two dimensional projection $(x_1, x_2, 0, 0)$ and the real Poincare section (i.e. values of displacements x_1 and x_2 at moments $t_n = 2\pi n/\omega$) needs to be projected on the chosen plane. The projection of attractor can be then in any place on the two dimensional cross-section, not necessarily within its basin of attraction.

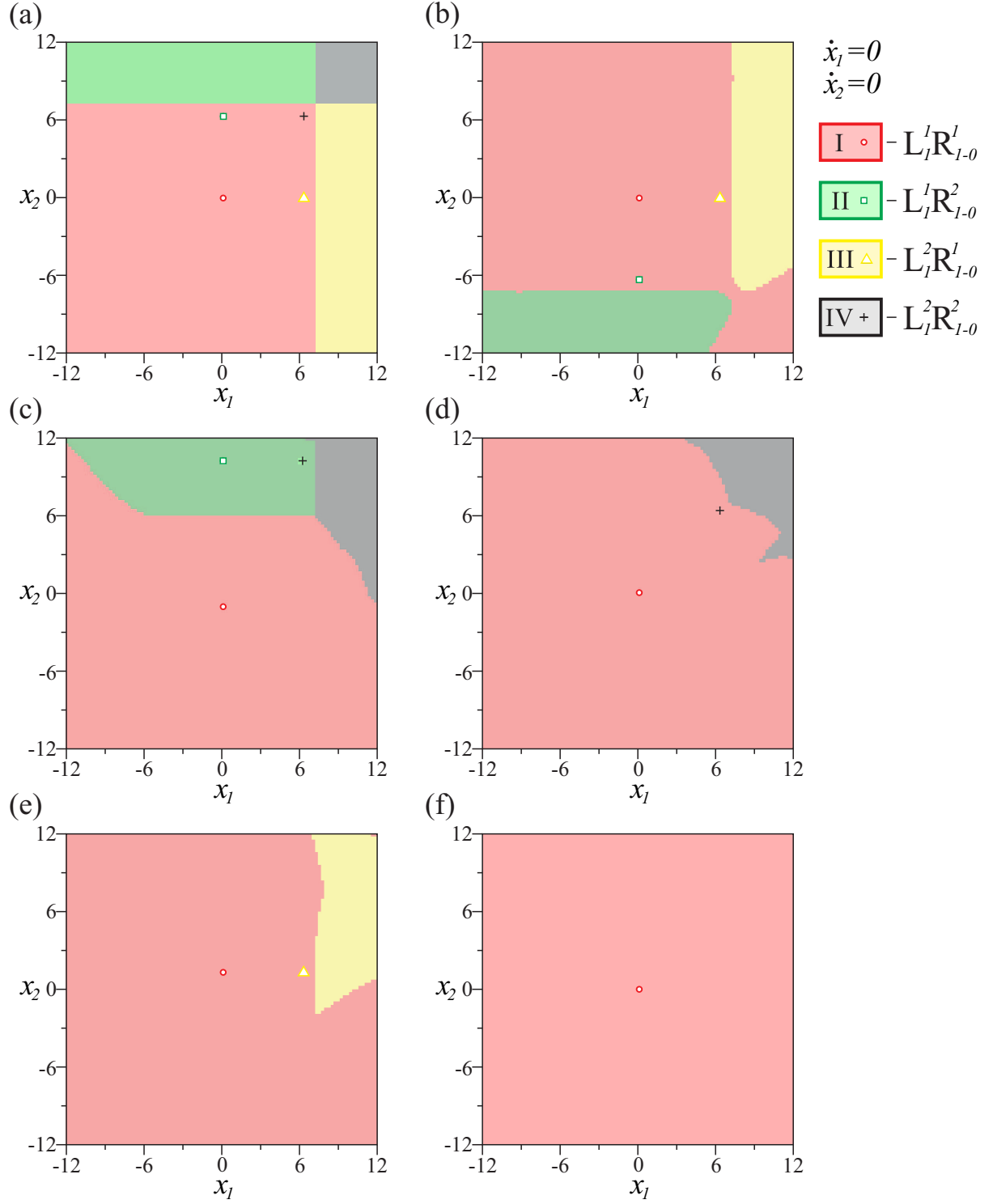


Figure 6: Basins of attraction for two Duffing oscillators for the following values of the system parameters $M = 1.0$, $k_1 = 1.0$, $k_2 = 0.01$, $c = 0.05$, $F = 1.0$, $\omega = 1.3$, $k_c = 8.0$, $c_c = 10.0$ for all subplots except subplot (c) for which $k_c = 10.0$, $c_c = 2.0$. The forcing phase shift and the distance between the oscillators are the following: (a) $\varphi = 0$, $d = 22$ (no impacts); (b) $\varphi = \pi$, $d = 15.0$; (c) $\varphi = 5.28$, $d = 10.5$; (d) $\varphi = 0$, $d = 6.0$; (e) $\varphi = 0.573\pi$, $d = 9$; (f) $\varphi = \pi$, $d = 5.0$. Attractors are marked as dots. Pairs of colours for given attractor and its basin are shown on right side of the figure.

Nevertheless, we do not resign from showing attractors because number of dots give information about the periodicity of the solution.

It is interesting to note that in all examples presented in Figure 6, only non impacting solutions were found and the number of them were controlled by the phase shift φ and the distance between the oscillators d . In general, as the distance decreases, the co-existence of the non impacting and impacting solutions becomes likely. For the small distances (below red line given in Figure 5(a)), only impacting solution(s) exist.

2.4. Bifurcation sequence

From practical point of view it is important to know the bifurcation scenarios of each solution. In this subsection we show how the destruction of non-impacting solutions occur when the distance between the oscillators d decreases for fixed value of φ (see Fig. 6). As in the considered system we have four non-impacting solutions we calculate four bifurcation diagrams. In the narrow range of d after destruction of non-impacting solutions we observe an existence of impacting solutions with small basins of attractions.

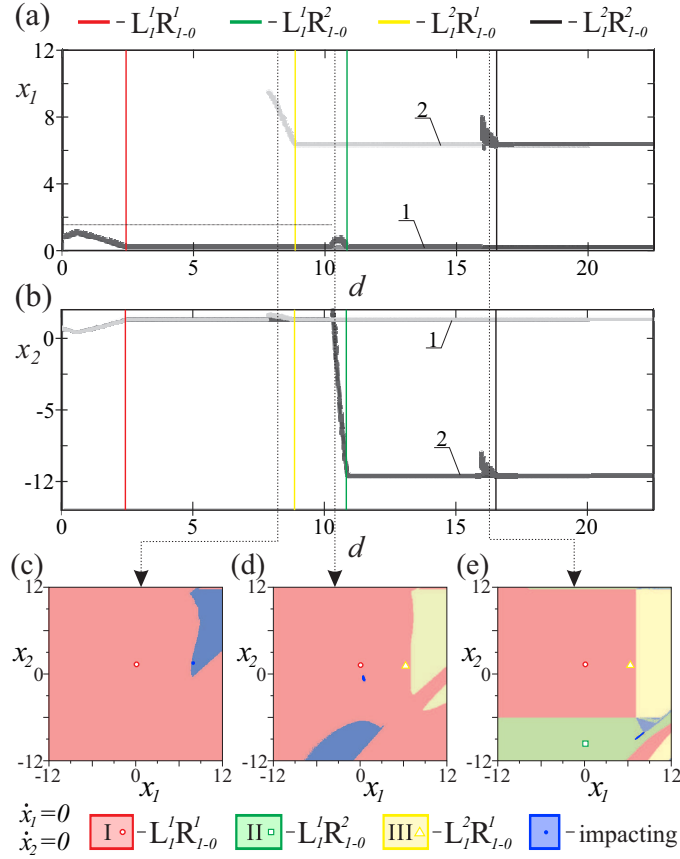


Figure 7: Bifurcation diagrams of left system L (a) and right system R (b) for four periodic non-impacting solutions versus distance d for $\varphi = 5/8\pi$, $c_c = 20$ and $k_c = 8$. Panes (c-e) show basins of attractions for marked values of distance d . i.e, $d = 8.2$ (c) $d = 10.25$ (d) and $d = 16.25$ (e). The blue colour indicates the attractors with impacts.

We fix the phase $\varphi = 5/8\pi$, stop parameters $k_c = 8.0$ and $c_c = 20.0$ and start our computation from $d = 22.5$. The results are presented in Figure 7(a,b). In Figure 7(a) we present the state of the left system (L), while in Figure 7(b) the state of the right system (R). We use vertical lines to mark when the destruction of given solution occurs (colours of lines correspond to the ones used in Figures 5 and 6). The first solution that is destabilized in grazing bifurcation for $d = 16.50$ (black line) is $L_1^2 R_{1-0}^2$. When further

decreasing d we observe a short transient impacting solution ($d \in [15.96, 16.5]$) and finally the transition to non-impacting solution $L_1^1 R_{1-0}^2$. Hence, then only three stable non-impacting solutions coexists. The second solution $L_1^1 R_{1-0}^2$ destabilizes in grazing bifurcation for $d = 10.85$ and after transient range it merges with $L_1^1 R_{1-0}^1$ for $d = 10.2$. Solution $L_1^2 R_{1-0}^1$ changes its stability in grazing bifurcation for $d = 8.8$ and merges with $L_1^1 R_{1-0}^1$ for $d = 7.85$. The last non-impacting solution ($L_1^1 R_{1-0}^1$) disappears, similarly to the mentioned before, in grazing bifurcation for $d = 2.45$ and we can observe only attractor with impacts. For all non-impacting solutions the destabilization is followed by the appearance of impacting solution which disappears when further decreasing the distance d .

In Figure 7(c-e) we show three basins of attractions calculated after the destabilization of non-impacting solutions for $d = 8.2$ (c) $d = 10.25$ (d) and $d = 16.25$ (e). We hold the same colours of basins of attraction as in Figure 6; additionally the blue colour indicates the basins of attraction of impacting solutions. In all three panels area of the blue basin is small comparing to the total area of the plot, i.e., panel (c) - 6.3%, panel (d) - 5.8% and panel (e) - 0.8%.

Although we are not able to completely avoid impacting solutions, they are only present for some small ranges of d close to destabilization of non-impacting solution and these range can be always decreased with proper tuning of stop parameters k_c and c_c . Moreover, even if the impacting solutions coexists their basins of attraction are not dominant.

3. Bi-linear oscillator

In this section we show that the behaviour presented for the system of two colliding Duffing oscillators is common for systems with impacts. Specifically, here it is demonstrated that with the properly chosen distance between the oscillators and difference in phase of the harmonic excitation, we can reduce the number of possible solutions. The same phenomenon was also observed in the coupled bi-linear systems shown in Figure 8. As in the previous case, when two oscillators remain at rest, they are separated by distance d , and the impacts which occur between them are of the soft type because of the presence of the spring with stiffness k_c and the viscous damper with damping coefficient c_c . Both oscillators have masses M and they are supported by the viscous dampers with damping coefficient c and by two linear springs of stiffnesses k_1 and k_2 which provide piecewise linear elastic resistance force. Springs with stiffness k_2 are separated from masses M by distance d_1 . Similarly to the Duffing systems, both oscillators are excited by harmonic force with amplitude F and frequency ω . Forcing of the first oscillator has fixed phase shift (equal to zero) while for the second one the phase shift is $\varphi \in (0, 2\pi)$ which is the control parameter of the coupled system.

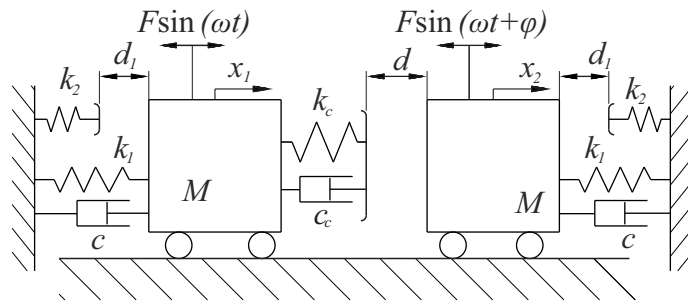


Figure 8: Model of two discontinuously coupled bi-linear oscillators.

The equations of motion for this coupled system are:

$$M\ddot{x}_1 + k_1 x_1 + k_2 (x_1 + d_1) H(-x_1 - d_1) + c\dot{x}_1 + F_C = F \sin(\omega t) \quad (4)$$

$$M\ddot{x}_2 + k_1 x_2 + k_2 (x_2 - d_1) H(x_2 - d_1) + c\dot{x}_2 - F_C = F \sin(\omega t + \varphi) \quad (5)$$

where $H(\cdot)$ is a Heaviside step function. Force generated by the discontinuous coupling (F_C) is given by the formula:

$$F_C = \begin{cases} 0 & \text{for } x_1 - x_2 < d \\ k_c ((x_1 - x_2) - d) + c_c (\dot{x}_1 - \dot{x}_2) & \text{for } x_1 - x_2 \geq d \end{cases} \quad (6)$$

The parameters have the following values: $M = 1.0 [kg]$, $k_1 = 1.0 [\frac{N}{m}]$, $k_2 = 29.0 [\frac{N}{m}]$, $c = 0.02 [\frac{Ns}{m}]$, $F = 0.518 [N]$, $\omega = 0.86 [\frac{1}{s}]$, $d_1 = 1.26 [m]$, $k_c = 8.0 [\frac{N}{m}]$, $c_c = 10.0 [\frac{Ns}{m}]$, $d = 1.0 [m]$.

Introducing non-dimensional time $\tau = t\omega_1$, where $\omega_1 = 1 [\frac{1}{s}]$, reference length $l_r = 1.0 [m]$ and mass $m_r = 1 [kg]$ we transform the equations (4) – (6) into non-dimensional form in which dimensional parameters are replaced by the following non-dimensional parameters:

$$M' = \frac{M}{m_r}, k'_1 = \frac{k_1 l_r}{m_r \omega_1^2}, k'_2 = \frac{k_2 l_r}{m_r \omega_1^2}, c' = \frac{c}{m_r \omega_1}, F' = \frac{F}{m_r l_r \omega_1^2}, \omega' = \frac{\omega}{\omega_1}, d'_1 = \frac{d_1}{l_r}, k'_c = \frac{k_c l_r}{m_r \omega_1^2}, c'_c = \frac{c_c}{m_r \omega_1}, d' = \frac{d}{l_r}.$$

Transformation to the dimensionless form was performed in the way that enables to hold the parameters' values, hence: $M' = 1.0$, $k'_1 = 1.0$, $k'_2 = 29.0$, $c' = 0.02$, $F' = 0.518$, $\omega' = 0.86$, $d'_1 = 1.26$, $k'_c = 8.0$, $c'_c = 10.0$. Distance between system d and phase shift in excitation φ are controlling parameters. For simplicity all of the primes used in definitions of dimensionless parameters will be omitted hereafter in the analysis.

It is well known that a single bi-linear oscillator exhibits a complex non-linear behavior [26] and the co-existing attractors are widespread phenomena in this system. A typical example of the basins of attractions for two co-existing solutions of a single bi-linear oscillator is presented in Figure 9 for $\omega = 0.86$ and $F = 0.518$. Here we observe two coexisting attractors; the first one is a period-2 response which period is twice longer than the period of the excitation. It is marked by red dots and its basin is given in orange colour. The second one is a period-5 response which is denoted by dark green squares and its basin is in green colour. Figure 9 displays that the basin of the period-2 solution is dominant.

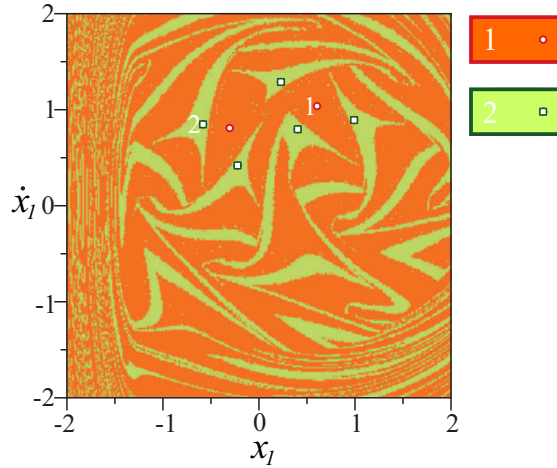


Figure 9: Basins of attraction for one bi-linear oscillator for $\omega = 0.86$ and $F = 0.518$. Two solutions are observed: with period 2 and period 5. ($M = 1.0$, $k_1 = 1.0$, $k_2 = 29.0$, $c = 0.02$, $d_1 = 1.26$)

Similarly as in the system of coupled Duffing oscillators, when we couple two bi-linear oscillators which have two co-existing solutions each, we observe many coexisting periodic states of the coupled system for large distant d . Let's fix the first system on the period-2 attractor. In such a case the second system has three possible states shown in Figure 10. The gray dots correspond to position of system at starting point and after the full period of excitation; the upper window and windows I and II the first part of the trajectory

is marked by black line and the second part is by grey line. In the first and the second solution ($L_2^1 R_{2-0}^1$ and $L_2^1 R_{2-1}^1$) both systems have period-2 responses. Hence, we can observe zero ($s = 0$) or one period of excitation shift ($s = 1$). In the third solution $L_2^1 R_{5-0}^2$ the second oscillator is on the period-5 attractor, hence the whole system has period 10 (smallest common denominator). As it easy to see, the following sequence of numbers in panel III in Figure 10 is the only possible solution because all possible pairs of numbers are present in the sequence (for details see Figure 2(a)).

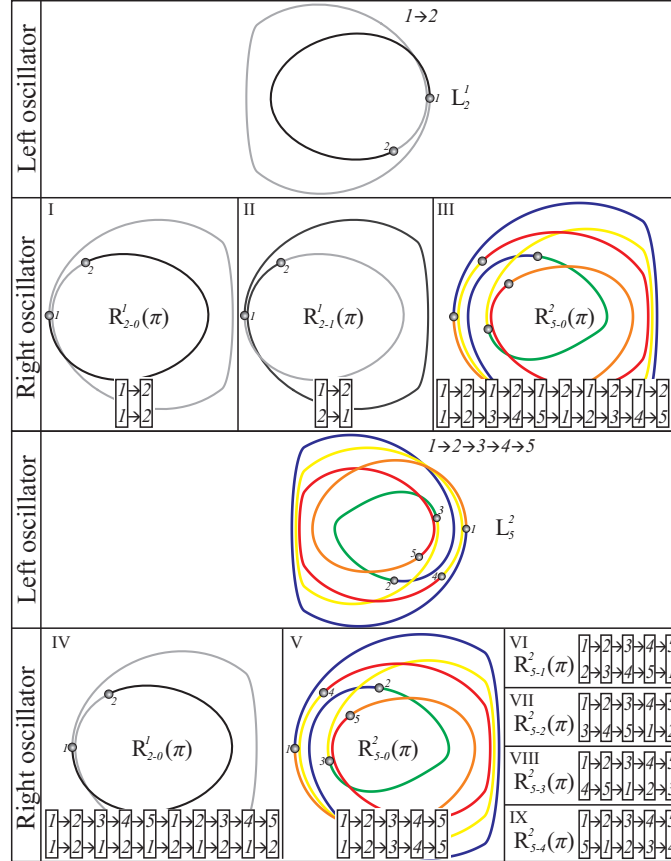


Figure 10: Nine possible solutions of the system that consists of two bi-linear oscillators. ($M = 1.0$, $k_1 = 1.0$, $k_2 = 29.0$, $c = 0.02$, $d_1 = 1.26$, $\omega = 0.86$, $F = 0.518$)

When the first system is on the period-5 attractor, we observe six possible solutions. The first one is a mirror solution of the one shown in the panel III in Figure 10, hence the second system exhibits the period-2 response. Next five solutions correspond to the case when both systems are on period-5 attractors, and as can be seen in panels V-IX in Figure 10, the phase of the second system solution can be either identical to the first one ($s = 0$, panel V), or shifted by 2π ($s = 1$, panel VI), 4π and so on up to $s = 4$ (panel IX). Therefore, for the considered system of two coupled bi-linear oscillators nine different non-impacting states are obtained.

Each of the above mentioned periodic states can be eliminated by the proper choice of the distance d and the phase shift of the excitation φ . The analysis shown in Figure 11 is presented in two parts for the clarity. In Figure 11(a) the red, blue and yellow lines correspond to following solutions: $L_2^1 R_{2-0}^1$, $L_2^1 R_{2-1}^1$ and $L_2^1 R_{5-1}^2$ and in Figure 11(b) the light blue, purple, pink, green, grey and orange lines to $L_5^2 R_{2-0}^1$, $L_5^2 R_{5-0}^2$, $L_5^2 R_{5-1}^2$, $L_5^2 R_{5-2}^2$, $L_5^2 R_{5-3}^2$ and $L_5^2 R_{5-4}^2$ respectively. Below all those lines we do not observe a given periodic non-impacting solution.

In Figure 12 four basins of attractions are presented for different values of d and φ . Basins in panel

(a) correspond to point (a) shown in Figure 11(a,b) with $d = 3.5$ and $\varphi = \pi$. In that case all possible non-impacting solutions are present in the system. In panel (b) (see (b) letter in Figure 11(a,b)) we have only two solutions $L_5^2 R_{2-0}^1$ and $L_5^2 R_{5-0}^2$. Two last panels are calculated for the pairs of d and φ for which only one state is present, i.e, (c) - $L_5^2 R_{2-0}^1$ and (d) $L_5^2 R_{5-0}^2$.

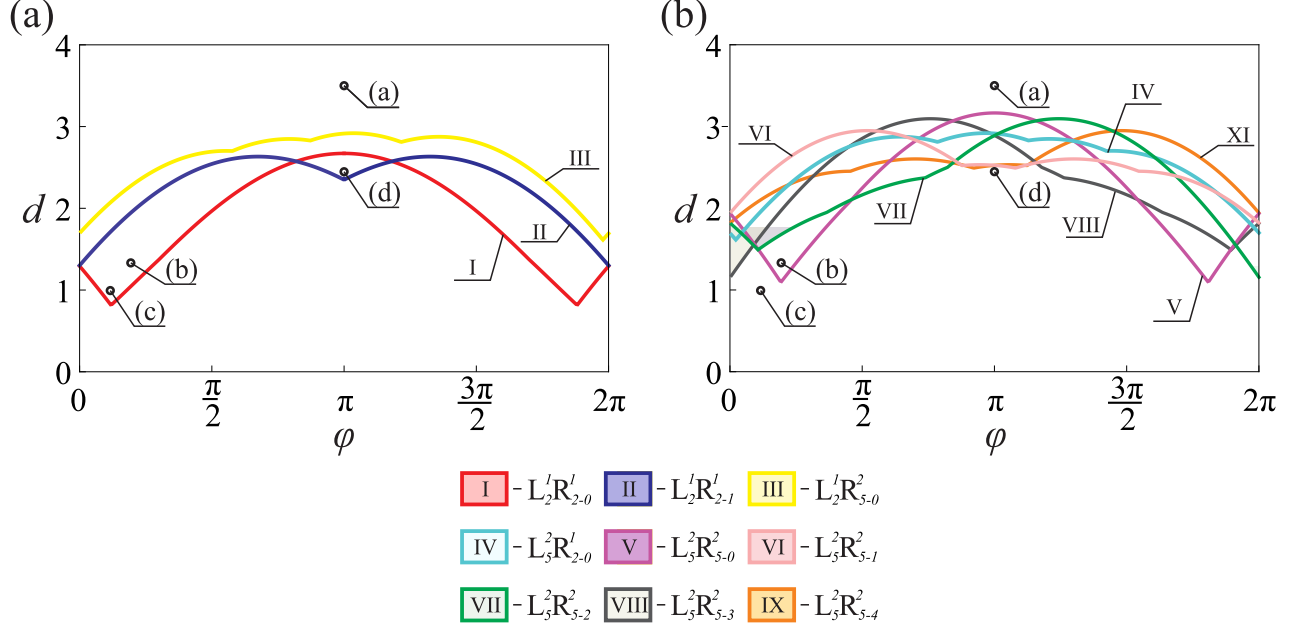


Figure 11: Possible solutions of the system that consists of two bi-linear oscillators in the (d, φ) plane. Each type of solution is marked and drawn with line of different color. ($M = 1.0$, $k_1 = 1.0$, $k_2 = 29.0$, $c = 0.02$, $d_1 = 1.26$, $\omega = 0.86$, $F = 0.518$)

The last example is shown in Figure 13. We change the frequency of excitation of bi-linear system to $\omega = 0.928$ and $F = 0.603$, which in the case of a single bi-linear oscillator gives us the coexistence of four different attractors, i.e., one with period one, two with period three and one with period five. For two discontinuously coupled oscillators at this frequency we observe 28 possible no-impacting solutions (see Figure 13(a)). As in the previous example with decreasing distance d and changing phase φ we can reduce the number of solutions. We do not show the whole analysis because it is similar to the one conducted in the previous cases. We focus on showing that by choosing two controlling parameters properly the number of solutions can be reduced to one as shown in Figure 13(b).

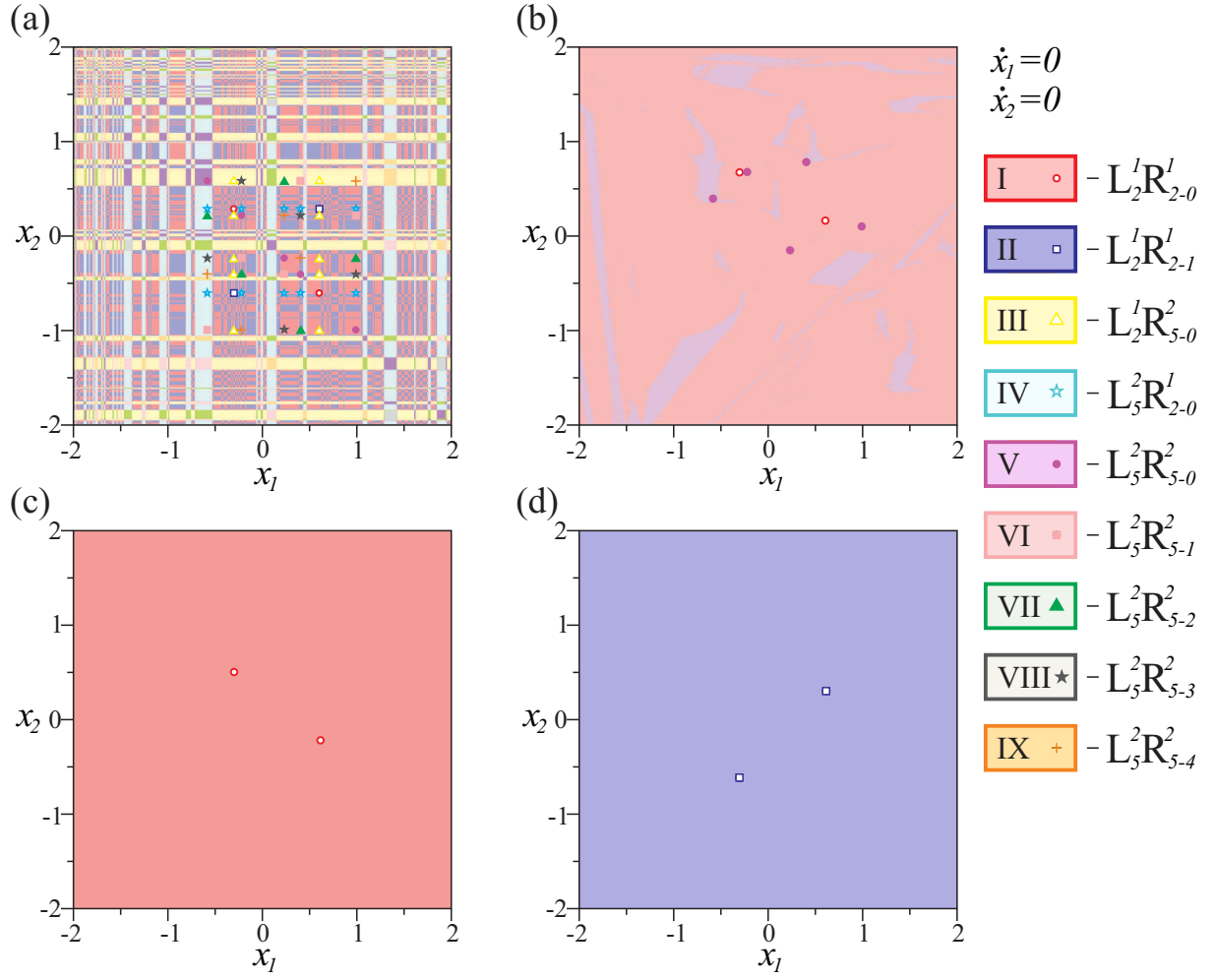


Figure 12: Basins of attraction for two bi-linear oscillators for $\omega = 0.86$, $F = 0.518$ and the following values of the system parameters $M = 1.0$, $k_1 = 1.0$, $k_2 = 29.0$, $c = 0.02$, $d_1 = 1.26$, $k_c = 8.0$, $c_c = 10.0$ for all subplots except subplot (d) for which $c_c = 2.0$. The forcing phase shift and the distance between the oscillators are the following: (a) $d = 10$ and $\varphi = \pi$ (no impacts); (b) $d = 1.332$ and $\varphi = 0.60916$; (c) $d = 1$ and $\varphi = 0.36424$; (d) $d = 2.448$ and $\varphi = \pi$. Attractors are marked as dots. Pairs of colours for given attractor and its basin are shown on right side of the figure.

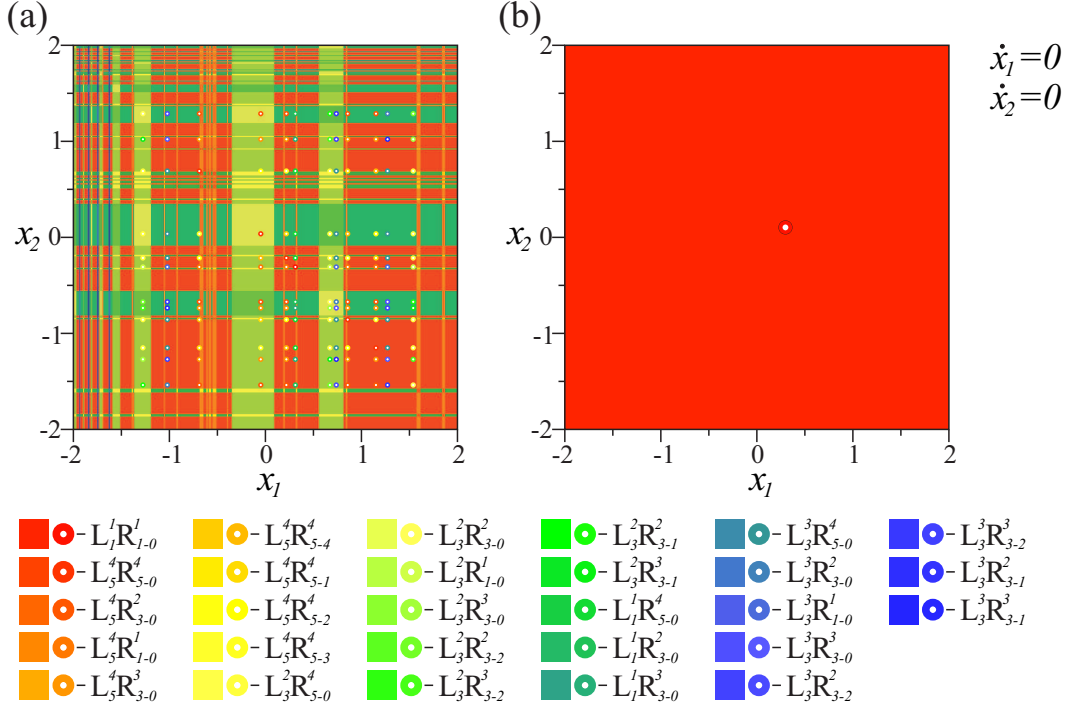


Figure 13: Basins of attraction for two bi-linear oscillators for $\omega = 0.928$ and $F = 0.602$ and the following values of the system parameters $M = 1.0$, $k_1 = 1.0$, $k_2 = 29.0$, $c = 0.02$, $d_1 = 1.26$, $k_c = 6.0$, $c_c = 5.0$. For given values of parameters single bi-linear oscillator has four coexisting attractors i.e., one period-1, two period-3 and one period-5. The forcing phase shift and the distance between the oscillators are the following: (a) $d = 10$ and $\varphi = \pi$ (no impacts) and (b) $d = 2$ and $\varphi = 0.4$. Attractors are marked as dots. Pairs of colours for given attractor and its basin are shown below the plots.

4. Coexistence of impacting and non-impacting solutions

In this section we show the coexistence of impacting and non-impacting solutions. The appearance of impacting solutions is probable close to the border where non-impacting solutions disappear. Such scenario occurs both for coupled bi-linear and Duffing systems. Near the threshold, for given d and φ one can observe the coexistence of impacting and non-impacting solutions but such case can be avoided by changing the parameters of the coupling which is shown in Fig. 14. In subplots (a) and (c) one can observe the coexistence of impacting and non-impacting attractors. For subplots (b,d) we changed coupling parameters so that only non-impacting solutions exist in the system. In part (b) we increase k_c from 8.0 to 20 and in part (d) we decrease c_c from 10 to 2.

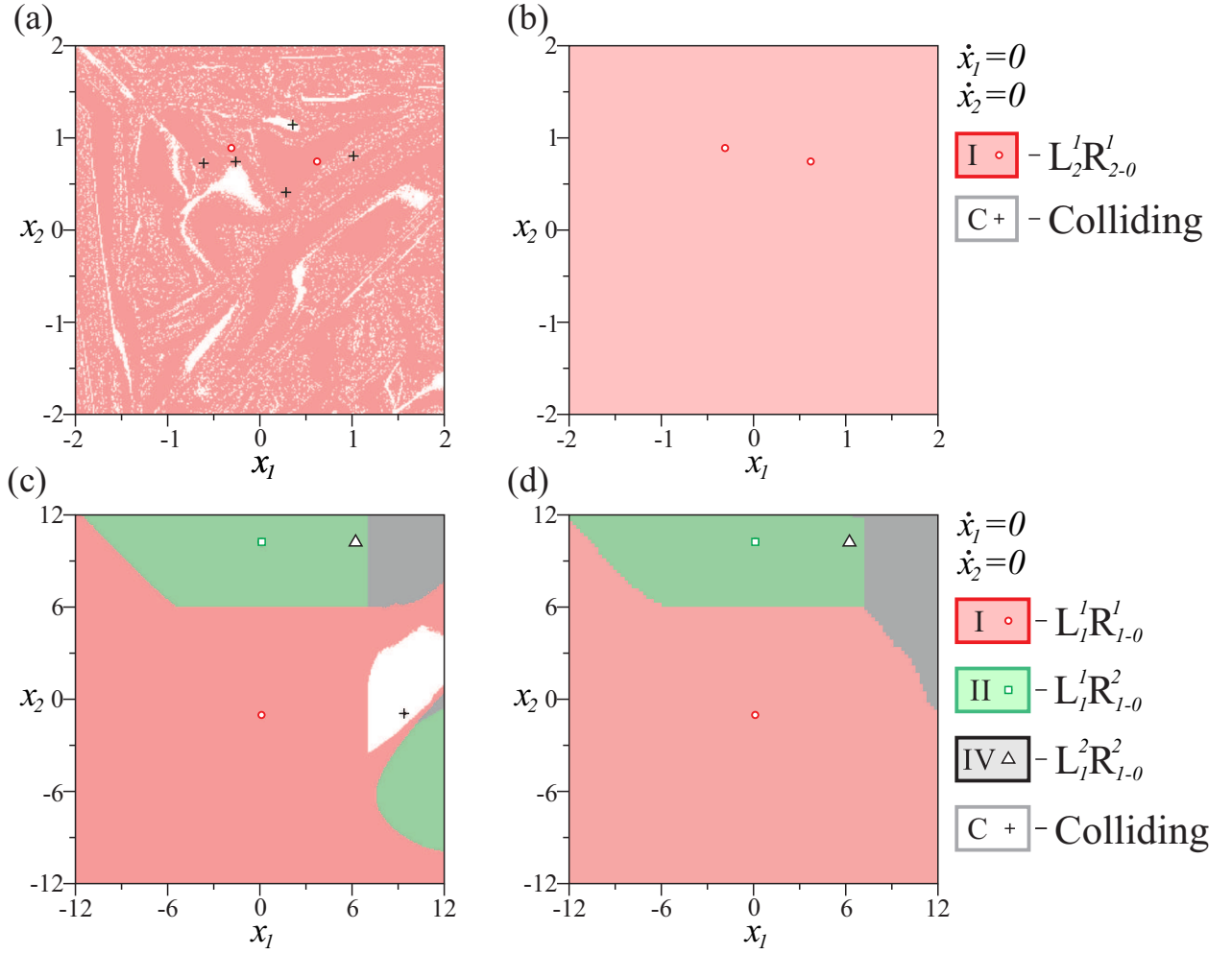


Figure 14: Basins of attraction for two bi-linear oscillators (a,b) and two Duffing oscillators (c,d). Subplots (a,b) were both calculated for the same system's parameters ($\omega = 0.86$, $F = 0.518$, $M = 1.0$, $k_1 = 1.0$, $k_2 = 29.0$, $c = 0.02$, $d_1 = 1.26$, $\varphi = 1.0$, $d = 1.5$) but different coupling parameters $k_c = 8.0$, $c_c = 10.0$ for subplot (a) and $k_c = 20.0$, $c_c = 10.0$ for subplot (b). Similarly subplots (c,d) were calculated for identical system's parameters ($\omega = 1.3$, $F = 1.0$, $M = 1.0$, $k_1 = 1.0$, $k_2 = 0.01$, $c = 0.05$, $\varphi = 5.28$, $d = 10.5$) and different coupling parameters: $k_c = 8.0$, $c_c = 10.0$ for subplot (c) and $k_c = 8.0$, $c_c = 2.0$ for subplot (d). Attractors are marked as dots. Pairs of colours for given attractor and its basin are shown on the left side of the figure.

From the practical point of view the crucial information is the knowledge how common is the coexistence of impacting and non-impacting solutions. The analysed systems are complex, hence we can use only numerical tools to predict how large is the basin of attraction of non-impacting solutions. To calculate this we use the method proposed by Menck et al. [27]. The idea behind it is simple, however it is a powerful tool to estimate the size of complex basins of attraction in multidimensional systems. Let us assume that we want to estimate the volume of basin of attraction \mathcal{B} of given attractor. To do it we measure the basin stability as $\mathcal{S}_{\mathcal{B} \cap \mathcal{Q}} = Vol \mathcal{B} \cap \mathcal{Q} / Vol \mathcal{Q} = [0, 1]$, where \mathcal{Q} is the subset of the state space that has finite volume. Thus, the system is integrated for N initial conditions drawn uniformly at random from \mathcal{Q} . Then, the number M of initial condition leading to the expected attractor is summarised and $\mathcal{S}_{\mathcal{B} \cap \mathcal{Q}} = M/N$. Number N in [27] is 500, in our case due to low dimensionality of phase space and discontinuity in system's equations we increase the number of trails to 1000. For each set of initial values we check the type of final attractor. Based on this the percentage distribution of solutions is determined. We want to estimate the participation of impacting solution, hence we do not distinguish their types but classify them all as the impacting ones. However, we calculate the percentage of each non-impacting solution. The ranges of initial conditions' values are taken

in the way to ensure that all considered attractors are within this multidimensional space, hence none of the attractors is predominant [28, 29]. Hence they are drawn from wide ranges and none of them have fixed value. In our calculations we want to show that the proper choice of coupling stiffness k_c or damping c_c results in elimination of impacting solutions (for the other parameters of the systems see captions).

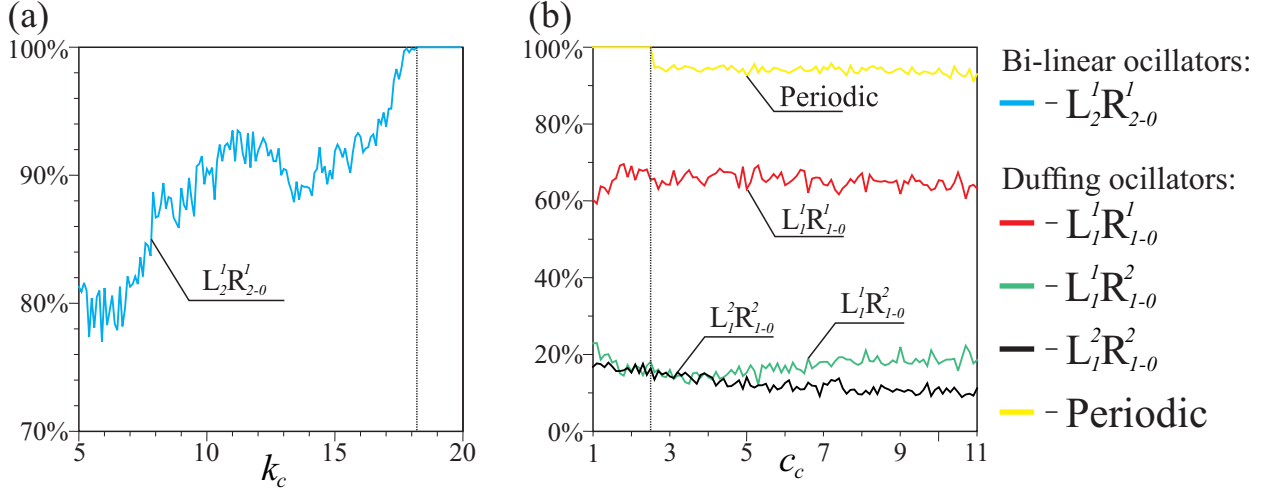


Figure 15: Changes of probability of reaching given attractor with the change of k_c parameter for bi-linear oscillators (a), and parameter c_c for Duffing oscillators (b). Colour of lines in subplots (a,b) correspond to the colours of the attractors presented in Fig. 14.

In Fig. 15(a) we show the plot for coupled bi-linear systems. For bi-linear systems the initial conditions $(x_{1,2}, \dot{x}_{1,2})$ are drawn from the range: $[-2, 2]$ and $k_c \in [5, 20]$. Values of d , φ and c_c are the same as in Fig. 14(a,b) and for this set of parameters only one non-impacting attractor exists. In the whole considered range of k_c the probability of occurrence of non-impacting solution is over 75% and with increasing of coupling stiffness it grows up to 100% for $k_c > 18.2$. The fluctuations along the probability curve are small (around 2%) and typical for complex, discontinuous systems with high sensitivity on initial conditions.

The same analysis is performed for coupled Duffing systems (see Fig. 15(b)). Here, all the initial conditions $(x_{1,2}, \dot{x}_{1,2})$ are drawn from range: $[-12, 12]$ and $c_c \in [1, 11]$. Values of d , φ and k_c are the same as in Fig. 14(c,d). For this set of parameters three non-impacting solutions exist, hence we show probability of each of them (colour of the line corresponds to the colour of the attractor on the basins plot). Moreover we calculate their sum to show the overall probability of reaching non-impacting solutions (yellow line). In case of Duffing systems the probability of reaching impacting solutions is low and does not exceed 9%. For low values of $c_c < 2.5$ the impacting solutions do not exist. The chance of achieving one of three non-impacting solutions stays nearly constant in the whole range of c_c .

The method presented above let us confirm the usefulness of the basins of attraction calculated for two-dimensional cross-sections of the four-dimensional phase space (presented in Figs. 6, 12, 13, 14). To authenticate that, we compare the probability of reaching given attractor obtained using both methods. For bi-linear oscillators we observe the full agreement. In Fig. 14(a), calculated using Dynamics, the chance to reach periodic attractor is 86%, while using Menck et al. method we obtain 85% chance. For parameters values used in Fig. 14(b) both methods give 100% chance of reaching periodic non-impacting solution (the only stable solutions in the whole phase space). For Duffing oscillators the difference in the results obtained using both methods is noticeable. For Fig 14(c) we have 69.5%, 21%, 5% and 4.5% chance for reaching $L_1^I R_{1-0}^I$, $L_1^I R_{1-0}^2$, $L_1^2 R_{1-0}^2$ and colliding solution respectively. Using Menck et. al. method we get 65.4%, 17.6%, 11.5% and 5.5%. Similar difference between both methods can be observed for Fig. 14(d): for solutions $L_1^I R_{1-0}^I$, $L_1^I R_{1-0}^2$, $L_1^2 R_{1-0}^2$ we get 75%, 17.5%, 7.5% chances using Dynamics, and 69.1%, 15.6%, 15.3% using Menck et. al. method. Hence, for Duffing oscillators we have up to 8% difference in the results obtained using both methods.

The good agreement of both methods for bi-linear systems is the result of the properties of basins of attraction of the single system. As can one see in Fig. 9 basin of attraction has a fractal structure, so with changing velocity there is no qualitative change of probability that we reach given attractor. For Duffing systems the basins of attraction for single oscillator has regular structure with sharp borders (see Fig. 3), hence with changing the velocity the chance of approaching given solution varies significantly (from 0% to 100%). This shows the main advantage of Menck et. al. method, where the initial conditions are generated from the whole accessible phase space.

5. Conclusions

In this paper we study the influence of discontinuous coupling on the dynamics of multistable systems. It is shown that with precise selection of the systems' parameters (the gap between the systems or/and phase shift of external excitation) one can easily decrease the number of coexisting solutions via discontinuous coupling. This idea is verified by performing calculation for two types of oscillators. The first system is composed of two Duffing oscillators, while the second one consists of two bi-linear oscillators. When systems are uncoupled ($\forall t \ (x_1 - x_2) < d$) there are numerous coexisting non-impacting solutions. When oscillators start to interact we observe impacts. Due to the damper in the stop the energy is dissipated and oscillators settle down on one of the non-impacting solutions and perform the synchronous motion (phase synchronization). The exchange of the energy (impacts) is a transient state lasting up to some minimal distance d for which only impacting solutions are presented. Near the threshold where non-impacting solutions destabilize, one can observe the coexistence of impacting and non-impacting solutions. However, by the exact selection of stop's parameters we are able to eliminate the impacting solutions. The proposed method is robust and the idea is likely to be applied in gear transmission systems, energy harvesters and in control and danger elimination of impacts between densely located oscillators or structures.

Acknowledgment

This work has been supported by Lodz University of Technology own Scholarship Fund (PB) and by Stipend for Young Outstanding Scientists from Ministry of Science and Higher Education of Poland (PP).

PB is supported by the Foundation for Polish Science (FNP).

References

- [1] J. J. Moreau and P. D. Panagiotopoulos *Nonsmooth Mechanics and Its Applications*, Springer Science & Business Media, Udine, 1988.
- [2] G. Gilardi and I. Sharf. Literature survey of contact dynamics modelling *Mechanism and Machine Theory* **37**, 1213 (2002).
- [3] B. Brogliato. *Nonsmooth mechanics: Models, dynamics and control*, Springer Science & Business Media, London, 1999
- [4] S. Hutzler, G. Delaney, D. Weaire and F. MacLeod. Rocking Newton's cradle. *American Journal of Physics* **72**, 1508 (2004).
- [5] B. Blazejczyk-Okolewska, K. Czolczynski, and T. Kapitaniak. Hard versus soft impacts in oscillatory systems modeling. *Communications in Nonlinear Science and Numerical Simulation*, **15**, 1358 (2010).
- [6] S. Kundu, S. Banerjee, and D. Giaouris. Vanishing singularity in hard impacting systems. *Discrete and Continuous Dynamical Systems - Series B* **16** 319 (2011).
- [7] T. Witelski, L. Virgin, and C. George. A driven system of impacting pendulums: Experiments and simulations *Journal of Sound and Vibration* **333**, 1734 (2014).
- [8] S. W. Shaw and P. J. Holmes. A periodically forced piecewise linear oscillator. *Journal of Sound and Vibration* **90**, 129 (1983).
- [9] U. Andreaus, L. Placidi, and G. Rega. Numerical simulation of the soft contact dynamics of an impacting bilinear oscillator. *Communications in Nonlinear Science and Numerical Simulation*, **15** 2603 (2010).
- [10] Y. Zhang, and K.D. Murphy. Multi-modal analysis on the intermittent contact dynamics of atomic force microscope. *Journal of Sound and Vibration*, **330** 5569 (2011).
- [11] W. Goldsmith. *Impact, the theory and physical behavior of colliding solids*. (Edward Arnold Pub. Ltd., London, 1964).
- [12] W. Serweta, A. Okolewski, B. Blazejczyk-Okolewska, K. Czolczynski, and T. Kapitaniak. Lyapunov exponents of impact oscillators with hertz's and newton's contact models. *International Journal of Mechanical Sciences* **89**, 194, (2014).
- [13] F. Peterka. Behaviour of impact oscillator with soft and preloaded stop. *Chaos, Solitons & Fractals* **18**(1), 79 (2003).

- [14] B. Banerjee, A. K. Bajaj, and P. Davies. Resonant dynamics of an autoparametric system: A study using higher-order averaging. *International Journal of Non-Linear Mechanics* **31**, 21 (1996).
- [15] M. Bernardo, C. Budd, A. R. Champneys, and P. Kowalczyk. *Piecewise-smooth dynamical systems: theory and applications*, (Springer, 2008).
- [16] A. Ganguli and S. Banerjee. Dangerous bifurcation at border collision: When does it occur?. *Physical Review E* **71**, 057202 (2005).
- [17] Y. Ma, M. Agarwal, and S. Banerjee. Border collision bifurcations in a soft impact system. *Physics Letters A* **354**, 281 (2006).
- [18] B. Blazejczyk-Okolewska, J. Brindley, K. Czołczynski, and T. Kapitaniak. Antiphase synchronization of chaos by noncontinuous coupling: two impacting oscillators. *Chaos, Solitons & Fractals* **12**, 1823 (2001).
- [19] A. Pikovsky, M. Rosenblum, and J. Kurths. *Synchronization. A Universal Concept in Nonlinear Sciences*. (Cambridge University Press, 2001).
- [20] S. H. Strogatz, D. M. Abrams, A. McRobie, B. Eckhardt, and E. Ott. Theoretical mechanics: Crowd synchrony on the millennium bridge. *Nature* **438**, 43 (2005).
- [21] P. Perlikowski, B. Jagiello, A. Stefanski, and T. Kapitaniak. Experimental observation of ragged synchronizability. *Physical Review E* **78**, 017203 (2008).
- [22] I.I. Blekhman, *Synchronization in Science and Technology*, ASME Press, New York, 1988.
- [23] H. Fujisaka and T. Yamada. Stability theory of synchronized motion in coupled oscillator systems. *Progress Theoretical Physics* **69**, 32, (1983).
- [24] M. G. Rosenblum, A. S. Pikovsky, and J. Kurths. Phase Synchronization of Chaotic Oscillators. *Physical Review Letters* **76**, 1804, (1996).
- [25] M. Kapitaniak, K. Czołczynski, P. Perlikowski, A. Stefanski, and T. Kapitaniak. Synchronous states of slowly rotating pendula. *Physics Reports* **541**, 1 (2014).
- [26] E. Pavlovskaja, J. Ing, M. Wiercigroch, and S. Banerjee. Complex dynamics of bilinear oscillator close to grazing. *International Journal of Bifurcation and Chaos* **20**, 3801 (2010).
- [27] P. J. Menck, J. Heitzig, N. Marwan, and J. Kurths. How basin stability complements the linear-stability paradigm. *Nature Physics* **9**, 89 (2013).
- [28] A. Chudzik, P. Perlikowski, A. Stefanski, and T. Kapitaniak. Multistability and rare attractors in van der Pol–Duffing oscillator. *International Journal of Bifurcation and Chaos* **21**, 1907 (2011).
- [29] P. Brzeski, M. Lazarek, T. Kapitaniak, J. Kurths, P. Perlikowski. Basin stability approach for quantifying responses of multistable systems with parameters mismatch. *ArXiv e-prints* **1602.03751**, (2016).